Editorial Manager(tm) for Apoptosis
Manuscript Draft

Manuscript Number: APPT567R1

Title: Cross-talk between two apoptotic pathways activated by endoplasmic reticulum stress: differential contribution of Caspase-12 and AIF

Article Type: Manuscript

Section/Category:

Keywords: AIF; caspase-12; thapsigargin; tunicamycin; endoplasmic reticulum

Corresponding Author: Valeria Marigo, Ph.D.

Corresponding Author's Institution: Telethon Institute of Genetics and Medicine

First Author: Daniela Sanges

Order of Authors: Daniela Sanges; Valeria Marigo, Ph.D.

Manuscript Region of Origin:

Cross-talk between two apoptotic pathways activated by endoplasmic reticulum stress: differential contribution of Caspase-12 and AIF

Daniela Sanges[1] and Valeria Marigo[1,2*]

[1] Telethon Institute of Genetics and Medicine (TIGEM), Naples, Italy

[2] Department of Biomedical Sciences, University of Modena and Reggio Emilia, Modena, Italy

[*] Corresponding author: Telethon Institute of Genetics and Medicine (TIGEM) via P. Castellino, 111 80131 Naples Italy. Tel: 081-6132216; Fax: 081-5609877; e-mail: marigo@tigem.it

Abbreviated title: cross-talk between caspase-12 and AIF in apoptosis

This work was supported in part by research grant from Fondazione Telethon and research grant EVI-GENORET: LSHG-CT-2 005-52036 from the European Community to V.M.

Abstract

Co-activation and cross-talk of different apoptotic pathways have been described in several systems however, the differential contributions of the different executors have not been well characterized. Here we report the co-translocation to the nucleus of caspase-12 and AIF in response to two endoplasmic reticulum (ER) stresses: protein misfolding and disruption of calcium homeostasis. As seen by treatment with pan-caspase inhibitor and calpain inhibitors, apoptosis is not mediated by executor caspases but by calpains. By reduction of AIF or caspase-12 expression we unraveled that AIF primarily controls apoptosis caused by changes in calcium homeostasis while caspase-12 has a main role in programmed cell death induced by protein misfolding. Nevertheless, the two apoptotic factors appear to reinforce each other during the apoptotic process, confirming that while the first response primarily involves one organelle, mitochondria and ER can influence each other in the apoptotic event.

Keywords: AIF; caspase-12; thapsigargin; tunicamycin; endoplasmic reticulum.

Introduction

Apoptosis can be activated through extrinsic or intrinsic pathways. Extrinsic pathways preferentially activate caspases that are cysteine proteases mediating apoptotic death in a variety of cellular systems. There are several examples of intrinsic pathways mediated by the mitochondria and, in response to apoptotic stimuli, several proteins are released from the intermembrane space of the organelle into the cytoplasm. Among them is cytochrome *c* that is involved in formation of the apoptosome, which leads to the activation of executor caspases [1]. Accumulating evidences suggest that other organelles, including the endoplasmic reticulum (ER) are also major points of integration of pro-apoptotic signaling. Each organelle possesses sensors that detect specific alterations, locally activates signal transduction pathways and emits signals that ensure inter-organellar cross-talk. The ER senses local stress through chaperones, Ca^{2+}-binding proteins and Ca^{2+} release channels, which can transmit ER Ca^{2+} responses to mitochondria.

Although caspases are frequently activated during cell death, in some cases caspase inhibition does not prevent apoptosis. A second family of proteases is the calpain family of calcium activated cysteine proteases [2]. Like caspases, they are synthesized as inactive pro-enzymes and can be autoprocessed to become active. Calpains are sensitive to increase of intracellular calcium levels for activation. Two ubiquitously expressed calpains are the isozymes μ-calpain and m-calpain, activated in vitro by micromolar and millimolar calcium concentrations respectively [3]. Calpains do not directly cause chromatin condensation but they are proteases that activate apoptotic factors.

Caspase-12 is a murine caspase belonging to the inflammatory caspase subgroup including caspase-1, -4, -5 and -11 [4]. Interestingly, caspase-12 has been linked to neuronal degeneration in neurotoxicity caused by amyloid-β protein [5], by prion protein [6] and in animal

models of ALS [7]. Caspase-12 is activated by m-calpain by elevated intracellular calcium in the presence of the pan-caspase inhibitor zVAD.fmk [8]. The cleaved active form of caspase-12 participates to the apoptotic event by translocation to the nucleus [9] or possibly through other caspases [6, 7]. Caspase-12 had been localized on the cytoplasmic side of the ER [5]. The observation that caspase-12 processing occurs during ER stress apoptosis has favored the idea that caspase-12 may be the initiator caspase during this process. However, absence of caspase-12 causes only a 12% reduction of ER stress apoptosis [5]. This evidence suggests that multiple mechanisms are operating during the apoptotic process.

Apoptosis-inducing factor (AIF) is a flavoprotein localized in the mitochondrial intermembrane space. It can exit the mitochondrion and directly translocate to the nucleus to execute DNA fragmentation that culminates in cell death [10]. Cleavage and release of AIF from mitochondria is regulated under some conditions by μ-calpain [11, 12]. AIF is able to mediate caspase-independent cell death because inhibition of caspase activation or activity does not always abolish AIF proapoptotic function [13]. It appears that there are several different mechanisms to release AIF from motochondria, either caspase dependent or independent [14]. Furthermore, the release of AIF from mitochondrion can occur independently from that of cytochrome *c* [15]. While AIF is much larger than cytochrome *c*, in several neuronal injury systems translocation of AIF to the nucleus was observed prior to the mitochondrial release of cytochrome *c* [15]. Finally, AIF activity can synergize and be enhanced by other factors like cyclophilin A [16].

In many pathological conditions apoptosis is activated through multiple pathways involving mitochondria and endoplasmic reticulum [8, 17-19]. The interdependence of multiple pathways is however not completely understood, and above all implication of executor caspases is still unclear. It is therefore very important to unravel interactions among different effectors of apoptosis that may be required to efficiently activate the apoptotic program. This

question is strictly related to development of therapeutic approaches to block apoptosis in diseases.

Our study was aimed at defining cross-talks between mitochondrial and ER localized apoptotic factors in different ER stress conditions. We show that caspase-12 and AIF concomitantly re-localize to the nucleus as a consequence of ER stress caused by tunicamycin treatment or by disruption of calcium homeostasis by thapsigargin treatment. Conversely, oxidative stress and Mn(II) caused activation of only one of the two factors. As seen by treatment with pan-caspase inhibitor or calpain inhibitors, ER-stress induced apoptosis is not mediated by caspases but by calpains. Finally we defined that downregulation of AIF prevents cell demise when calcium homeostasis is disrupted by thapsigargin. On the other hand, caspase-12 has a primary role in apoptosis caused by ER stress induced by protein misfolding.

Materials and Methods

Cell culture and treatments

NIH3T3 fibroblasts were grown in DMEM supplemented with 10% FBS, penicillin (100U/ml) and streptomycin (50μg/ml) at 37°C in a 5% CO_2 atmosphere.

Apoptosis was induced by treatments with H_2O_2 (400μM) for 12h, $MnCl_2$ (1μM) for 48h, thapsigargin (2μM; SIGMA, Milan, Italy) for 48h, tunicamycin (2μg/ml; SIGMA, Milan, Italy) for 48h. Cells were pre-treated with calpain inhibitor I (ALLN, N-Ac-L-L-norleucinal, 25μM; Calbiochem, Darmstadt, Germany), calpain inhibitor II (ALLM, N-Ac-L-L-M-CHO, 5μM; Calbiochem, Darmstadt, Germany), calpastatin (20μM; Calbiochem, Darmstadt, Germany), zVAD.fmk (N-benzyloxycarbonyl-Val-Ala-Asp-fluoromethylketone, 50μM; SIGMA, Milan, Italy) for 30min before apoptosis induction.

Immunofluorescence

Cells were fixed with 4% paraformaldehyde in PBS at room temperature for 30 min and washed in PBS. Samples were permeabilized with permeabilization buffer (0.1M NaCitrate, 0.1% Triton X-100) for 2 min at 4°C and then blocked for 30 min in blocking buffer (3% BSA, 20% FBS, 0.5M Tris-HCl pH7.5). Apoptotic nuclei were detected by TdT-dUTP terminal nick-end labeling kit (TUNEL,fluorescein; Roche Diagnostics, Monza, Italy) according to the manufacturer's protocols. Samples were then incubated overnight with primary antibodies for immunohistochemistry procedure. The primary antibodies used were: rabbit anti-AIF (1:100; SIGMA, Milan, Italy), rat anti caspase-12 (1:100; SIGMA, Milan, Italy), goat anti ERAB (1: 100; Santa Cruz biotechnology inc., Santa Cruz, CA, USA) and mouse anti cytochrome c (1:200; Promega Italia, Milan, Italy). After incubation for 45 minutes with secondary Cy5 anti-rabbit (Jackson Immunoresearch, West Grove, PA, USA) and Alexa Fluor® 568 anti-rat and anti-rabbit antibodies (Molecular Probes, Eugene, OR, USA), slides were coverslipped with Vectashield (Vector laboratories, Burlingame, CA, USA) and photographed using either an Axioplan microscope (Zeiss) or a Leica Laser Confocal Microscope System.

Protein fractionation and western blotting

Cells were harvested in PBS and lysed in lysis buffer (50mM Tris-HCl pH 8.0, 1% NP-40, 0.25% Na-deoxycholate, 150mM NaCl, 1mM EDTA, 1mM PMSF, aprotinin, leupeptin, pepstatin 1µg/ml each). When nucleus enriched lysates were prepared, cells were transferred to a 2ml Dounce homogenizer with 200µl of cold homogenizing buffer (20mM Hepes-KOH pH 7.5, 250mM sucrose, 10mM KCl, 1.5mM $MgCl_2$, 1mM EDTA, 1mM EGTA, 1mM DTT, 1mM PMSF, aprotinin, leupeptin, pepstatin 1µg/ml each) and incubated 30 min on ice. Plasma membrane was disrupted with 20 strokes and the nuclear fraction was isolated by

centrifugation at 900xg for 10 min at 4°C. The pellet was washed twice in cold homogenizing buffer and resuspended in lysis buffer. The purity of nuclear enriched lysates was controlled by western blot analysis using a specific nuclear marker (anti-acetyl-Histone H3 1:1000; SIGMA, Milan, Italy), the mitochondrial marker ATP synthase α subunit (C5, 1:1000, Molecular Probes, Eugene, OR, USA), and a cytosol marker (anti-actin, 1:1000, Santa Cruz Biotechnology, Santa Cruz, CA, USA).

Equivalent amounts of protein extracts (60μg), as determined by the Bradford method (Bio-Rad Italy, Segrate, Italy), were resolved using SDS-PAGE and western blot analysis was performed following standard procedures. The antibodies used were: rabbit anti-AIF (1:400; Oncogene Research Products, San Diego, CA, USA), rabbit anti-caspase-12 (1:1000; Cell Signaling Technology, Beverly, MA, USA), anti-caspase-3 active (1:500; SIGMA, Milan, Italy), anti caspase-9 (1: 500; SIGMA, Milan, Italy), anti-βtubulin (1:2500; SIGMA, Milan, Italy).

shRNA constructs and clones

Two sequences beginning with an AA dinucleotide were chosen in the *caspase-12* mRNA: 5'-AATGATGAGGATGATGGACCT and 5'- AACCCAAGATTCTCATCATGC and designed two hairpin RNAi template oligonucleotides:

sense sequence I:

5'GATCCCCAATGATGAGGATGATGGACCTTTCAAGAGAAGGTCCATCATCCTCATCATTTTTTTGGAAC;

sense sequence II:

5'GATCCCCAACCCAAGATTCTCATCATGCTTCAAGAGAGCATGATGAGAATCTTGGGTTTTTTTTGGAAC.

Control hairpin RNAi template oligonucleotide for sequence I was generated by mutagenizing 3 nucleotides (in bold) in the targeting sequence (underlined):

Control caspase-12 sense sequence I:

5'GATCCCCAATG**C**C**G**CGGATGATGGACCTTTCAAGAGAAGGTCCATCATCC**GC**G**G**CATTTTTTTGGAAC;

AIF hairpin siRNA template oligonucleotides were designed as previously reported [20]. As control we mutated 3 nucleotides in the targeting sequence (shown in bold):

5'GATCCCCTT**C**TTCT**T**AG**A**AATGGCGTGTTCAAGAGACACGCCATT**T**CT**A**GAA**G**A ATTTTTGGAAC.

Sense and antisense oligonucleotides were annealed to form a hairpin siRNA template insert and cloned into the pSUPER vector (OligoEngine, Seattle, WA) using BglII/XhoI restriction sites. The insert was checked by sequencing. The template insert was then cloned into pRNAT-U6.1/neo vector using two external sites (EcoRI and KpnI). Stable transfection of shRNA vector was performed in NIH3T3 cells with the Polyfect transfection reagent (Qiagen, Milan, Italy) following the manufacturer's protocol. Stable transfected clones were selected with G418 (1mg/ml).

Calcium ion concentration measurement

NIH3T3 cells were exposed to different stress stimuli and at different time points after treatment Fluo-4 AM (Molecular Probes, Eugene, OR, USA) was loaded into cells for 30 min at 37°C in calcium free medium. Cells were then washed in PBS and slides were coverslipped with Vectashield (Vector laboratories, Burlingame, CA, USA). Analysis was performed on 20 sequential layers of each cell at 488nm with a Leica Laser Confocal Microscope System. Images were then analyzed with the Leica confocal software (LCS). The

fluorescence average intensity (mean amplitude) of each area was measured. The average amplitude of 20 cells was reported as histogram.

RT-PCR

Total RNA from tunicamycin and thapsigargin treated cells was extracted by the TRIzol® methods (Gibco-BRL, Milan, Italy) at different time points. RT-PCR was performed in a two-step protocol using SuperScript™ II reverse transcriptase and Taq gold polymerase. The number of the cycles and the annealing temperature were adjusted depending on the gene amplified. Primers for RT-PCR analysis of CHOP/Gadd153 and GRP78/Bip expression were: GADDfw 5'TGCCTTTCTCCTTCGGGACAC and GADDrev 5' GTGACCTCTGCTGGTTCTGGC; BIPfw 5'GATAATCAACCAACTGTTAC and BIPrev 5'GTATCCTCTTCACCAGTTGG reverse. RT-PCR were normalized with GAPDH using as primers: 5'TGAAGGTCGGAGTCAACGGATTTG and 5'CATGTGGGCCATGAGGTCCACCAC.

Results

Based on recent evidences reporting co-activation of multiple apoptotic pathways during cell demise, we investigated interaction between AIF and caspase-12 pathways in two different apoptotic conditions: disregulation of Ca^{2+} homeostasis and protein misfolding. We used thapsigargin that inhibits ER-associated Ca^{2+}-ATPase and disrupts Ca^{2+} homeostasis [21]. We found that NIH3T3 murine fibroblasts respond to thapsigargin stress undergoing apoptosis as detected by TUNEL staining (Figure 1F and P). Thapsigargin causes release of AIF from the mitochondria and translocation to the nucleus (Figure 1D). Nuclear localization was also confirmed by immunoblotting detecting AIF in nuclear fractions of thapsigargin stressed cells (57kD as previously reported [10], Figure 1Q). Thapsigargin treatment also activated caspase-

12 that changed its subcellular localization from the ER to the nucleus (Figure 1E). Caspase-12 is activated by cleavage (35kD and 42kD, as previously reported [9]) and translocates to the nucleus (Figure 1F and Q). Tunicamycin is a specific inhibitor of N-glycosylation and inducer of ER stress [5]. We similarly detected co-localization of AIF and caspase-12 inside the nuclei of cells undergoing apoptosis after tunicamycin treatment (Figure 1G-I and P and Q). Interestingly, we observed that thapsigargin causes a fast change in intracellular calcium within 6 hours after treatment (Figure 2A) while protein misfolding responses are activated only after 24 hours (Figure 2B). On the other hand, tunicamycin upregulates protein misfolding response factors within 12 hours (Figure 2B), while calcium concentration in the cells only slightly increased at the same time point (Figure 2A).

We observed translocation of the two apoptotic factors in the same apoptotic cells as demonstrated by triple staining for TUNEL, AIF and caspase-12 (inserts in Figure 1D-I). Specificity of nuclear translocation of the two factors was demonstrated by confocal analysis of either a mitochondrial protein (cytochrome c in figure 2 C-K) or an ER marker (ERAB in figure 2L-T). Neither cytochrome c nor ERAB showed nuclear localization in these conditions. Co-localization of AIF and caspase-12 was not observed after H_2O_2 treatment that caused only translocation of AIF to the nucleus, as previously reported [14], but no activation of caspase-12 (Figure 1J-L, P and Q). On the other hand, Mn(II) induced mitochondria-independent apoptosis via caspase-12 [22] without release of AIF (Figure 1M-O, P and Q). While H_2O_2 activates caspase-3 and caspase-9, active fragments of these two executor caspases were not detectable after treatment with thapsigargin and tunicamycin (Figure 1R). These data showed for the first time co-localization of AIF and caspase-12 in the apoptotic nuclei. We also demonstrated that AIF and caspase-12 translocate to the nucleus in response to several apoptotic conditions, yet their co-localization appears to be a specific response to ER stress.

To confirm lack of involvement of executor caspases, shown by immunoblotting in figure 1R, we exposed thapsigargin and tunicamycin treated cells to pan-caspase inhibitor zVAD.fmk. zVAD.fmk did not protect NIH3T3 cells from cell death, while it was effective on H_2O_2 treated cells (Figure 3A). Calpains have been previously reported to activate independently caspase-12 and AIF [8, 11]. We therefore exposed thapsigargin treated cells to either calpain inhibitor I (ALLN) or calpain inhibitor II (ALLM) or a mixture of both. We calculated a reduction of 60% of thapsigargin induced apoptotic cells by treatment with ALLM, while ALLN appeared to be more efficient in blocking apoptosis (reduction to 10%). In tunicamycin treated cells ALLM showed a stronger inhibitory activity. The mixture of both ALLM and ALLN completely blocked apoptosis in both conditions (Figure 3A). We confirmed involvement of calpains by treating the cells with the calpastatin peptide, a specific inhibitor of calpains, able to block apoptosis induced by thapsigargina and tunicamycin (Figure 3A). We observed concomitant translocation of AIF and caspase-12 in cells undergoing apoptosis after treatment with caspase inhibitor but not in cells treated with the different calpain inhibitors (Figure 3C-Z). Western blot analysis confirmed that calpain inhibitors and calapstatin but not zVAD.fmk were efficiently blocking translocation of AIF and caspase-12 (Figure 3B).

The observation that no thapsigargin or tunicamycin-treated cell showed single AIF or single caspase-12 relocalization to the nucleus suggested a direct cooperation of AIF and caspase-12 in activating apoptosis initiated by ER stress. However, experiments presented so far did not allow to address whether apoptosis required the concomitant presence of AIF together with caspase-12 inside the nucleus. Otherwise the two pathways could act independently or could cooperate to activate cell death. To address this issue we generated NIH3T3 clones in which either expression of AIF or caspase-12 was repressed by RNA interference. Two different targeting sequences were chosen in the caspase-12 mRNA and

both shRNAs were able to efficiently knock-down caspase-12 expression (Figure 4K and data not shown). Figure 4 shows AIF and caspase-12 protein levels (tested by immunofluorescence and immunoblotting) in the interfered clones, clones 1 and 2 were chosen for AIF^- experiments, clones 1 and 6 were used for caspase-12^- experiments. Mutagenized targeting sequences were used (see Materials and Methods) as controls and these shRNAs did not affect expression of either protein (Figure 4B, G and K contr.).

Absence of AIF completely abolished apoptosis induced by thapsigargin (Figure 5A, C-N and Table 1). Interestingly, we observed nuclear localization of caspase-12 in 24% of the AIF^- cells treated with thapsigargin (Figure 5A and Table 1). These cells are not positive to TUNEL staining (Figure 5 F-H, arrow). When we treated AIF^- cells with thapsigargin together with calpain inhibitors we blocked caspase-12 translocation to the nucleus (Figure 5A-N). By counting the number of nuclei stained with caspase-12, we observed that ALLM alone could prevent caspase-12 activation similarly to the mixture of the ALLM and ALLN or to calpastatin peptide (Figure 5A and Table 1). As control, we treated AIF^- cells with H_2O_2 and all cells underwent apoptosis but caspase-12 was never found in the nucleus (Table 1). On the contrary, caspase-12 was always found inside the nucleus in AIF^- apoptotic cells treated with Mn(II) or tunicamycin (Figure 5A, O-Z and Table 1). These data suggested that AIF mediates apoptosis caused by disruption of Ca^{2+} homeostasis, while it is dispensable when apoptosis is activated either by oxidative stress or by protein misfolding. The observation of caspase-12 inside the nucleus of TUNEL negative AIF^- cells suggested that caspase-12 activation does not strictly correlate with apoptosis. In tunicamycin treated cells lack of AIF caused only partial reduction of apoptosis (20% versus 50%). All cells undergoing apoptosis showed caspase-12 localization to the nucleus (Figure 5A, R-T and Table 1). Interestingly, 3% of AIF^- cells were stained by TUNEL even in the absence of apoptotic stimuli but caspase-12 was never detected in these nuclei (Figure 5A and Table 1).

This finding is not surprising, in fact absence of AIF was previously correlated with reduction of respiratory activity and cell death [23, 24].

We then treated caspase-12$^-$ cells with thapsigargin and analyzed AIF subcellular localization. Downregulation of caspase-12 in NIH3T3 cells partially protected the cells from apoptosis in fact only 30% of the cells underwent programmed cell death (Figure 6A and Table 1). In all apoptotic cells we detected nuclear localization of AIF (Figure 6F-H, arrow). As expected caspase-12$^-$ cells underwent apoptosis when stressed with H_2O_2 and AIF always translocated to the nucleus (Table 1). Caspase-12$^-$ cells were otherwise resistant to Mn(II) stress and tunicamycin treatment (Figure 6A, O-Z and Table 1). Apoptosis caused by thapsigargin could be significantly reduced in caspase-12$^-$ cells by treatment with calpain inhibitors, blocking also AIF relocalization (Figure 6A-B, C-N and Table 1). Otherwise, zVAD.fmk did not protect caspase-12$^-$ cells from thapsigargin induced programmed cell death (Figure 6A and Table 1). Similar results were observed with both shRNAs targeting caspase-12 (data not shown). To confirm the effects that we observed in AIF$^-$ and caspase-12$^-$ cells were specific for the knock-down of the these factors, we performed similar experiments with a mutagenized shRNA (see Materials and Methods and figure 4). Cells expressing mutagenized shRNAs behaved like wild type cells (Figure 5A and 6A blue bars, and 5B and 6B). All these data were confirmed by western blotting on nuclear enriched extracts purified from AIF$^-$ and Caspase-12$^-$ cells (Figures 5B and 6B). We also treated cells with thapsigargin and tunicamycin for prolonged time points (up to 72 hours) and we did not observe increased percentages of apoptotic cells in AIF$^-$ and caspase-12$^-$ cells (data not shown).

Discussion

In this paper we describe for the first time the cross-talk between two apoptotic pathways activated by ER stress when Ca^{2+} homeostasis and protein folding are disrupted. In these

conditions we observed translocation of AIF and caspase-12 to the nucleus. We also observed that in both apoptotic conditions interference with calpain activity blocks activation of the two factors. Calpains are calcium activated proteases and therefore intracellular Ca^{2+} concentration may play an important role in both apoptotic conditions. The mechanism through which thapsigargin alters calcium homeostasis is known [1], but tunicamycin treatment that affects N-glycosylation and protein folding may as well increase intracellular Ca^{2+}. Protein misfolding and accumulation in the ER were previously reported to stimulate calcium influx [25]. Furthermore, we also observed an increase in intracellular Ca^{2+} as a consequence of tunicamycin treatment. Initiation of these two pathways appears to be mediated by calpains, calcium dependent proteases, and not by caspases. In fact, we did not detect activated caspase-3 and caspase-9 and pancaspase inhibitor zVAD.fmk was unable to prevent apoptosis. Otherwise, calpain inhibitors were able to completely block cell death. Recently, no activation of AIF and caspase-12 was reported in a neuronal cell line exposed to tunicamycin [26]. Those experiments were performed in a neuronal immortalized cell line by treating the cells with higher concentrations of the drug. This may activate different responses as also suggested by the very fast activation of GADD153 (6 hours) compared to the conditions applied in this study (activation of GADD153 can be detected only after 24 hours).

The most interesting and novel finding reported in this paper is the differential contribution of ER released caspase-12 and mitochondrial released AIF in the two apoptotic conditions. By decreasing expression of either AIF or caspase-12 we defined that AIF is necessary for activation of apoptosis induced by thapsigargin while caspase-12 has a fundamental function when cell death is triggered by tunicamycin. Activated caspase-12 was anyway detected in the absence of AIF inside some nuclei that were not TUNEL positive. This observation implies that caspase-12 activation and translocation to the nucleus is not completely dependent on AIF, conversely it appears to be, at least partially, a direct response

to calpains. This is based on data showing that treatment with different calpain inhibitors is able to prevent caspase-12 activation in AIF$^-$ cells. Secondly, translocation to the nucleus of caspase-12 does not necessarily activate apoptosis. These data are in agreement with previous reports describing that caspase-12 may be dispensable for the execution of cell death after ER stress [5, 27]. On the same line, we showed that downregulation of caspase-12 was partially beneficial to cells treated with thapsigargin. In the absence of caspase-12 we observed a strict correlation of cell demise with AIF translocation to the nucleus, and this is also dependent on calpain activity. These data unraveled a fundamental role of AIF in induction of cell death in conditions altering calcium homeostasis and the reduction of apoptosis in the absence of caspase-12 implies at least a partial contribution of this apoptotic factor.

On the other hand, tunicamicyn induced programmed cell death strongly correlates with caspase-12 activity and was less dependent on the function of AIF. In fact, absence of caspase-12 prevented apoptosis and AIF translocation to the nucleus. Conversely, lack of AIF merely reduced the number of apoptotic cells. Furthermore, nuclear caspase-12 is found in every single AIF$^-$ apoptotic cell treated with tunicamycin. These data revealed a direct correlation of tunicamycin induced ER stress apoptosis with caspase-12 activation.

We observed cell death in 3% of AIF$^-$ cells, even without stress agents. We could otherwise expect that lack of AIF, a mitochondrial protein with oxidoreductase activity [23], may influence the ability of cells to undergo apoptosis. On the contrary, apoptosis was detected in AIF$^-$ cell exposed to H_2O_2 excluding an increased resistance due to a difference in their bioenergetic condition.

All together these data suggest that different apoptotic factors act as *primus movens* of the apoptotic cascades activated either by changes of Ca^{2+} homeostasis or protein misfolding. We also observed a reinforcing function of these two apoptotic factors between each other. We propose a model to describe these observations (Figure 7). In the presence of thapsigargin

the first change in the cell is the increase of intracellular Ca^{2+} concentration [1] (Figure 7A). This appears to have a stronger effect on the release and activation of AIF from the mitochondria. In fact, in the absence of AIF cells do not undergo apoptosis and there is a strict correlation of AIF translocation to the nucleus and activation of apoptosis in caspase-12^- cells. However, the percentage of cells activating AIF is reduced when caspase-12 is absent. This indicates that caspase-12 itself or a downstream factor can reinforce AIF activation in these detrimental conditions. Secondly, we observed that increased intracellular Ca^{2+} directly caused caspase-12 translocation inside AIF^- nuclei. However, not all the cells activate caspase-12 suggesting that AIF itself acts as a positive signal for this activation. In addition, the effective block of cell death by calpain inhibitors suggested that calpains are probably the proteases controlling activation of both factors. Figure 7B shows a schematic representation of the cell treated with tunicamycin. Protein misfolding appears to have a direct role on caspase-12 activation and release from the ER. In fact a complete preservation from cell death and AIF activation was observed in caspase-12^- cells. Furthermore, in this condition AIF activation appears to be dependent on caspase-12 or on an intermediate still unknown signal downstream of it. We suggest that calpains are probably involved also in protein misfolding activated cell death because calpain inhibitors can block apoptosis. Based on the observation that lack of AIF partially preserves cells from apoptosis, we suggest that caspase-12 is probably the first response to protein misfolding but to effectively initiate apoptosis it activates other effectors such as AIF. On the other hand, lack of AIF reduces but not prevents apoptosis reinforcing the hypothesis that this pathway is probably activated also by other effectors. We have not identified yet the factors involved in the cross talk of the two pathways. Calcium itself may play a role. It is also known that Bax and Bak can sense ER damage and function on mitochondrial membrane permeabilization [28].

Conclusions

In summary, here we reported for the first time co-activation of AIF and caspase-12 as apoptotic responses to two ER stress conditions. The novel finding of this study is that changes in intracellular calcium activate AIF together with caspase-12 but AIF is necessary for this response. Interestingly, we showed caspase-12 translocation to the nucleus even in the absence of chromatin condensation. These data suggest that caspase-12 relocalization to the nucleus does not necessarily correlate with DNA fragmentation. On the other hand, AIF is not required for protein misfolding induced apoptosis while, in this case, caspase-12 has a primary function both on AIF activation and cell death. Therefore, we unraveled interactions of mitochondrial and ER apoptotic factors in ER stress induced cell demise. Future studies will be focusing on defining key players at the intersection of these different apoptotic pathways.

Acknowledgements

The authors wish to thank Dr E.I. Rugarli and C. Missero for sharing reagents and discussion of data. S. Arbucci and the Open Laboratory Core (TIGEM-IGB) for confocal microscopy.

References

1. Ferri KF and Kroemer G. Organelle-specific initiation of cell death pathways. Nat Cell Biol 2001; 3: E255-63.

2. Wang KK. Calpain and caspase: can you tell the difference? Trends Neurosci 2000; 23: 20-6.

3. Croall DE and DeMartino GN. Calcium-activated neutral protease (calpain) system: structure, function, and regulation. Physiol Rev 1991; 71: 813-47.

4. Lamkanfi M, Declercq W, Kalai M, Saelens X and Vandenabeele P. Alice in caspase land. A phylogenetic analysis of caspases from worm to man. Cell Death Differ 2002; 9: 358-61.

5. Nakagawa T, Zhu H, Morishima N, et al. Caspase-12 mediates endoplasmic-reticulum-specific apoptosis and cytotoxicity by amyloid-beta. Nature 2000; 403: 98-103.

6. Hetz C, Russelakis-Carneiro M, Maundrell K, Castilla J and Soto C. Caspase-12 and endoplasmic reticulum stress mediate neurotoxicity of pathological prion protein. Embo J 2003; 22: 5435-45.

7. Wootz H, Hansson I, Korhonen L, Napankangas U and Lindholm D. Caspase-12 cleavage and increased oxidative stress during motoneuron degeneration in transgenic mouse model of ALS. Biochem Biophys Res Commun 2004; 322: 281-6.

8. Nakagawa T and Yuan J. Cross-talk between two cysteine protease families. Activation of caspase-12 by calpain in apoptosis. J Cell Biol 2000; 150: 887-94.

9. Fujita E, Kouroku Y, Jimbo A, et al. Caspase-12 processing and fragment translocation into nuclei of tunicamycin-treated cells. Cell Death Differ 2002; 9: 1108-14.

10. Susin SA, Lorenzo HK, Zamzami N, et al. Molecular characterization of mitochondrial apoptosis-inducing factor. Nature 1999; 397: 441-6.

11. Polster BM, Basanez G, Etxebarria A, Hardwick JM and Nicholls DG. Calpain I induces cleavage and release of apoptosis-inducing factor from isolated mitochondria. J Biol Chem 2005; 280: 6447-54.

12. Liou AK, Zhou Z, Pei W, et al. BimEL up-regulation potentiates AIF translocation and cell death in response to MPTP. Faseb J 2005; 19: 1350-2.

13. Daugas E, Susin SA, Zamzami N, et al. Mitochondrio-nuclear translocation of AIF in apoptosis and necrosis. Faseb J 2000; 14: 729-39.

14. Arnoult D, Parone P, Martinou JC, et al. Mitochondrial release of apoptosis-inducing factor occurs downstream of cytochrome c release in response to several proapoptotic stimuli. J Cell Biol 2002; 159: 923-9.

15. Cande C, Vahsen N, Garrido C and Kroemer G. Apoptosis-inducing factor (AIF): caspase-independent after all. Cell Death Differ 2004; 11: 591-5.

16. Cande C, Vahsen N, Kouranti I, et al. AIF and cyclophilin A cooperate in apoptosis-associated chromatinolysis. Oncogene 2004; 23: 1514-21.

17. Doonan F, Donovan M and Cotter TG. Activation of Multiple Pathways during Photoreceptor Apoptosis in the rd Mouse. Invest Ophthalmol Vis Sci 2005; 46: 3530-8.

18. Jayanthi S, Deng X, Noailles PA, Ladenheim B and Cadet JL. Methamphetamine induces neuronal apoptosis via cross-talks between endoplasmic reticulum and mitochondria-dependent death cascades. Faseb J 2004; 18: 238-51.

19. Kitamura Y, Miyamura A, Takata K, et al. Possible involvement of both endoplasmic reticulum-and mitochondria-dependent pathways in thapsigargin-induced apoptosis in human neuroblastoma SH-SY5Y cells. J Pharmacol Sci 2003; 92: 228-36.

20. Yuan CQ, Li YN and Zhang XF. Down-regulation of apoptosis-inducing factor protein by RNA interference inhibits UVA-induced cell death. Biochem Biophys Res Commun 2004; 317: 1108-13.

21. Thastrup O, Cullen PJ, Drobak BK, Hanley MR and Dawson AP. Thapsigargin, a tumor promoter, discharges intracellular Ca2+ stores by specific inhibition of the endoplasmic reticulum Ca2(+)-ATPase. Proc Natl Acad Sci U S A 1990; 87: 2466-70.

22. Oubrahim H, Chock PB and Stadtman ER. Manganese(II) induces apoptotic cell death in NIH3T3 cells via a caspase-12-dependent pathway. J Biol Chem 2002; 277: 20135-8.

23. Klein JA, Longo-Guess CM, Rossmann MP, et al. The harlequin mouse mutation downregulates apoptosis-inducing factor. Nature 2002; 419: 367-74.

24. Vahsen N, Cande C, Briere JJ, et al. AIF deficiency compromises oxidative phosphorylation. Embo J 2004; 23: 4679-89.

25. Bonilla M, Nastase KK and Cunningham KW. Essential role of calcineurin in response to endoplasmic reticulum stress. Embo J 2002; 21: 2343-53.

26. Di Sano F, Ferraro E, Tufi R, et al. Endoplasmic Reticulum Stress Induces Apoptosis by an Apoptosome-dependent but Caspase 12-independent Mechanism. J Biol Chem 2006; 281: 2693-2700.

27. Kalai M, Lamkanfi M, Denecker G, et al. Regulation of the expression and processing of caspase-12. J Cell Biol 2003; 162: 457-67.

28. Zong WX, Li C, Hatzivassiliou G, et al. Bax and Bak can localize to the endoplasmic reticulum to initiate apoptosis. J Cell Biol 2003; 162: 59-69.

Legends to figure

Figure 1. Co-activation of AIF and caspase-12 after thapsigargin and tunicamycin treatments.

A-O: Fluorescent microscopy of NIH3T3 cells double stained with anti-AIF (A, D, G, J and M, green) and anti-caspase-12 antibodies (B, E, H, K and N, red). Cells were stressed with 2μM thapsigargin (TG) for 48 hours, 2μg/ml tunicamycin (TM) for 48 hours, 400μM hydrogen peroxide (H_2O_2) for 12 hours, 1μM $MnCl_2$ ($MnCl_2$) for 48 hours or not stressed (untr.). Merged images of AIF and caspase-12 staining are shown in C, F, I, L and O where DAPI staining labels nuclei in blue. Scale bar: 10 μm. Inserts are confocal images of the thapsigargin or tunicamycin treated NIH3T3 cells triple stained with anti-AIF (blue in D and G), anti-caspase-12 (red in E and H) and TUNEL (green in F and I). Merged confocal images are shown in F and I (inserts, MERGE). Co-localization of AIF, caspase-12 and TUNEL was confirmed by confocal microscopy (inserts).

P: Statistical analysis of apoptosis (TUNEL positive nuclei, green bars) and nuclear translocation of AIF (blue bars) and caspase-12 (red bars). Values are shown as percentage of stained nuclei versus the number of total nuclei.

Q: Western blot analysis of AIF and caspase-12 in nuclear enriched lysates purified from NIH3T3 cells either untreated (untr.) or treated with hydrogen peroxide (H_2O_2), manganesium chloride ($MnCl_2$), thapsigargin (TG) and tunicamycin (TM). The amounts of protein were normalized with western blotting of the nuclear protein marker acetyl-histone-3 (H3). Contamination of the nuclear enriched lysates was checked with a mitochondrial protein marker (C5) and cytoskeleton marker actin. Last lane on the right (untr.) shows total cell lysates analyzed with the same antibodies. In total lysates of untreated cells the anti-caspase-12 antibody detects the uncleaved 57kD protein.

R: Western blot analysis of activated caspase-3 and caspase-9 in total protein lysates purified from untreated (untr.) and treated NIH3T3 cells. The amounts of protein were normalized with the nuclear protein marker acetyl-histone-3 (H3).

Figure 2. Changes in intracellular calcium and activation of protein misfolding response after thapsigargin and tunicamycin treatments

A: Analysis of intracellular calcium in either untreated (untr.) NIH3T3 cells or treated with 2μM thapsigargin (black bars) or 2μg/ml tunicamycin (white bars) for 6, 12, 24 and 48 hours. Fluorescence intensity was reported as the mean amplitude of 20 different transversal layers of 20 cells.

B: RT-PCR expression analysis of two protein misfolding sensor genes: CHOP/Gadd153 and GRP78/Bip. NIH3T3 cells were treated with 2μM thapsigargin (TG) and 2μg/ml tunicamycin (TM) for 12, 24 and 48 hours. RT-PCR was normalized with GAPDH.

C-K: confocal microscopy of NIH3T3 cells either untreated (untr.) or treated with 2μM thapsigargin (TG) or 2μg/ml tunicamycin (TM) for 48 hours and double stained with antibodies anti-mitochondrial marker cytochrome c (CYT-C, red in C, F and I) and anti-AIF (AIF, green in D, G and J). Merged images are shown in E, H and K.

L-T: confocal microscopy of NIH3T3 cells either untreated (untr.) or treated with 2μM thapsigargin (TG) or 2μg/ml tunicamycin (TM) for 48 hours and double stained with antibodies anti-ER marker ERAB (red in L, O and R) and anti-caspase-12 (casp-12, green in M, P and S). Merged images are shown in N, Q and T.

Figure 3. Translocations of AIF and caspase-12 are blocked by calpain-inhibitors.

A: Statistical analysis of cell death of NIH3T3 cells pre-treated with either pan-caspase inhibitor (zvad, 50μM) or with calpain-inibitors I (alln, 25μM), II (allm, 5μM), calpain-

inibitors I and II (alln-allm) or calpastatin (castn, 20μM) and then exposed to either 2μM thapsigargin (TG) or 2μg/ml tunicamycin (TM) for 48 hours or 400μM H_2O_2 for 12 hours. Percentages of cell death (%) were calculated as number of TUNEL-positive nuclei versus total number of nuclei.

B: Western blot analysis of AIF and caspase-12 on nuclear enriched lysates purified from NIH3T3 cells either untreated (untr.) or treated with thapsigargin (TG) or tunicamycin (TM) in the presence of pan-caspase-inhibitor (casp.inh) or calpain-inhibitors I and II (calp.inh) or calpastatin (castn). The amounts of protein were normalized with the nuclear protein marker acetyl-histone-3 (H3).

C-N: Confocal microscopy of thapsigargin treated NIH3T3 cells in the absence (C-E) or presence of caspase inhibitor (F-H) or calpain-inhibitors (I-K) or calapstatin peptide (L-N) shows that calpain-inhibitors and calpastatin prevent AIF and caspase-12 translocation to the nucleus (arrows).

O-Z: Confocal microscopy of tunicamycin treated NIH3T3 cells in the absence (O-Q) or presence of caspase inhibitor (R-T) or calpain-inhibitors (U-W) or calapstatin peptide (X-Z) shows that calpain-inhibitors and calpastatin prevent AIF and caspase-12 translocation to the nucleus (arrows).

Figure 4. Characterization of AIF$^-$ and caspase-12$^-$ stable NIH3T3 clones

A-E: Immunofluorescence with AIF antibody on wild type (non transf.), control RNAi (contr. AIF) and stable AIF knock-down RNAi clones (#1, #2, #3). Scale bar: 10 μm.

F-J: Immunofluorescence with caspase-12 antibody on wild type (non transf.), control RNAi (contr. Casp-12) and stable caspase-12 knock-down RNAi clones (#1, #4, #6).

Cells were photographed with the same exposure time (1000 ms).

K: Western blot analysis of AIF and caspase-12 expression on protein lysates purified from AIF$^-$ stable clones #1, #2 and #3 and caspase12$^-$ stable clones #1, #4 and #6. In the first lane protein lysates from control wild type cells (non transf.) and in the second lane control shRNAs were analyzed (contr. AIF and contr. Casp-12). The amount of protein was normalized with the β-tubulin antibody.

Figure 5. Analysis of caspase-12 translocation in AIF$^-$ stable clones.

A: Statistical analysis of apoptisis (TUNEL positive, blue bars for control RNAi and green bars for AIF$^-$ RNAi) and caspase-12 nuclear translocation (red bars) in stable clones obtained with AIF specific shRNA (green and red bars) and AIF control shRNA (blue bars).

B: Western blotting of AIF and caspase-12 in nuclear enriched lysates from stable clones obtained with AIF control shRNA (contr.) and with AIF specific shRNA. Clones were either untreated (untr.) or treated with 2μM thapsigargin for 48 hours in the absence or presence of calpain inhibitors (calp. inh.) and calpastatin (castn). Western blotting was normalized by analysis of nuclear acetyl-histone-3 (H3).

C-N: Immunofluorescence of AIF$^-$ stable clone #1 treated with 2μM thapsigargin (TG) in the absence or presence of calpain inhibitors (calp. inh.) and calpastatin peptide (castn) and double stained with TUNEL (C, F, I and L) and caspase-12 antibody (D, G, J and M). Merged images with DAPI are shown in E, H, K, N. Arrow in H shows a TUNEL-negative cell with nuclear localization of caspase-12.

O-Z: Immunofluorescence of AIF$^-$ stable clone #1 treated with 2μg/ml tunicamycin (TM) in the absence or presence of calpain inhibitors (calp. inh.) and calpastatin (castn) and double stained with TUNEL (O, R, U and X) and caspase-12 antibody (P, S, V and Y). Merged images with DAPI are shown in Q, T, W, Z.

Figure 6. Analysis of AIF translocation in caspase-12$^-$ stable clones.

A: Statistical analysis of apoptotic cells (TUNEL positive, blue bars for control RNAi and green bars for caspase-12$^-$ RNAi) and AIF nuclear translocation (red bars) in stable clones obtained with caspase-12 specific shRNA (green and red bars) and caspase-12 control shRNA (blue bars).

B: Western blotting of AIF and caspase-12 in nuclear enriched lysates from stable clones obtained with caspase-12 control shRNA (contr.) and with caspase-12 specific shRNA. Clones were either untreated (untr.) or treated with thapsigargin (TG) or tunicamycin (TM) in the absence or presence of calpain inhibitors (calp. inh.) and calpastatin peptide (castn). Western blotting was normalized by analysis of nuclear acetyl-histone-3 (H3).

C-N Immunofluorescence of caspase-12$^-$ stable clone #1 treated with 2μM thapsigargin (TG) for 48 hours in the absence or presence of calpain inhibitors (calp. inh.) and calpastatin peptide (castn) and double stained with TUNEL (C, F, I and L) and AIF antibody (D, G, J and M). Merged images with DAPI are shown in E, H, K, N. Arrow in H shows a TUNEL-positive cell with nuclear localization of AIF.

O-Z Immunofluorescence of caspase-12$^-$ stable clone #1 treated with 2μg/ml tunicamycin (TM) for 48 hours in the absence or presence of calpain inhibitors (calp. inh.) and calpastatin peptide (castn) and double stained with TUNEL (O, R, U and X) and AIF antibody (P, S, V and Y). Merged images with DAPI are shown in Q, T, W, Z.

Figure 7. Interaction between AIF and caspase-12 apoptotic pathways.

A: Thapsigargin treatment inhibits ER-associated Ca^{2+}-ATPase and increases intracellular Ca^{2+}. AIF has a prevalent role on the cell death program (thick arrow) but caspase-12 either directly or indirectly positively reinforces this pathway (dashed arrows).

B: Caspase-12 is necessary for the apoptotic process together with AIF activation in response to protein misfolding (thick arrow). AIF activation downstream to caspase-12 can be either a direct or indirect response (dashed arrows).

Table 1. Statistical analysis on AIF$^-$ and caspase 12$^-$ clones after thapsigargin and tunicamycin treatments

treatment	apoptotic AIF$^-$	AIF$^-$ / nuclear caspase 12	apoptotic caspase 12$^-$	caspase 12$^-$ / nuclear AIF	wt
untreated	3	0	0	0	0
zvad	3	0	-	-	-
alln allm	3	0	-	-	-
TG	3	24	30	30	98
TG zvad	3	24	30	30	98
TG alln	3	15	3	3	10
TG allm	3	0	6	6	40
TG alln allm	3	0	2	2	1
TG castn	3	0	0	0	0
TM	20	20	0	0	50
TM zvad	20	20	0	0	50
TM alln	14	14	0	0	30
TM allm	3	2	0	0	7
TM alln allm	3	0	0	0	0
TG castn	3	0	0	0	0
H_2O_2	99	0	97	97	98
$MnCl_2$	91	91	1	0	92

All the values are represented as the percentage of TUNEL positive cells versus total number of the cells. Mean values have been calculated by three counts of three different experiments.

Figure 1

Click here to download high resolution image

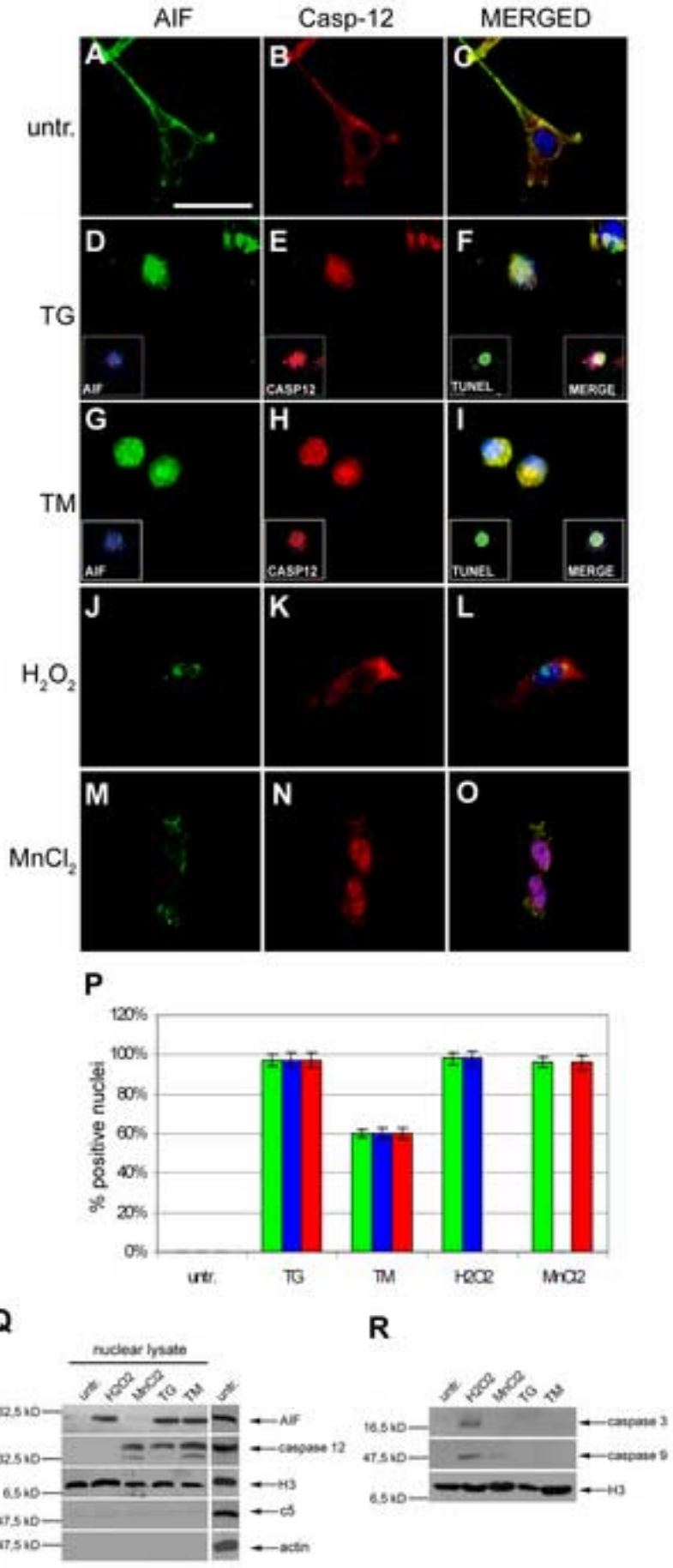

Figure 2

Click here to download high resolution image

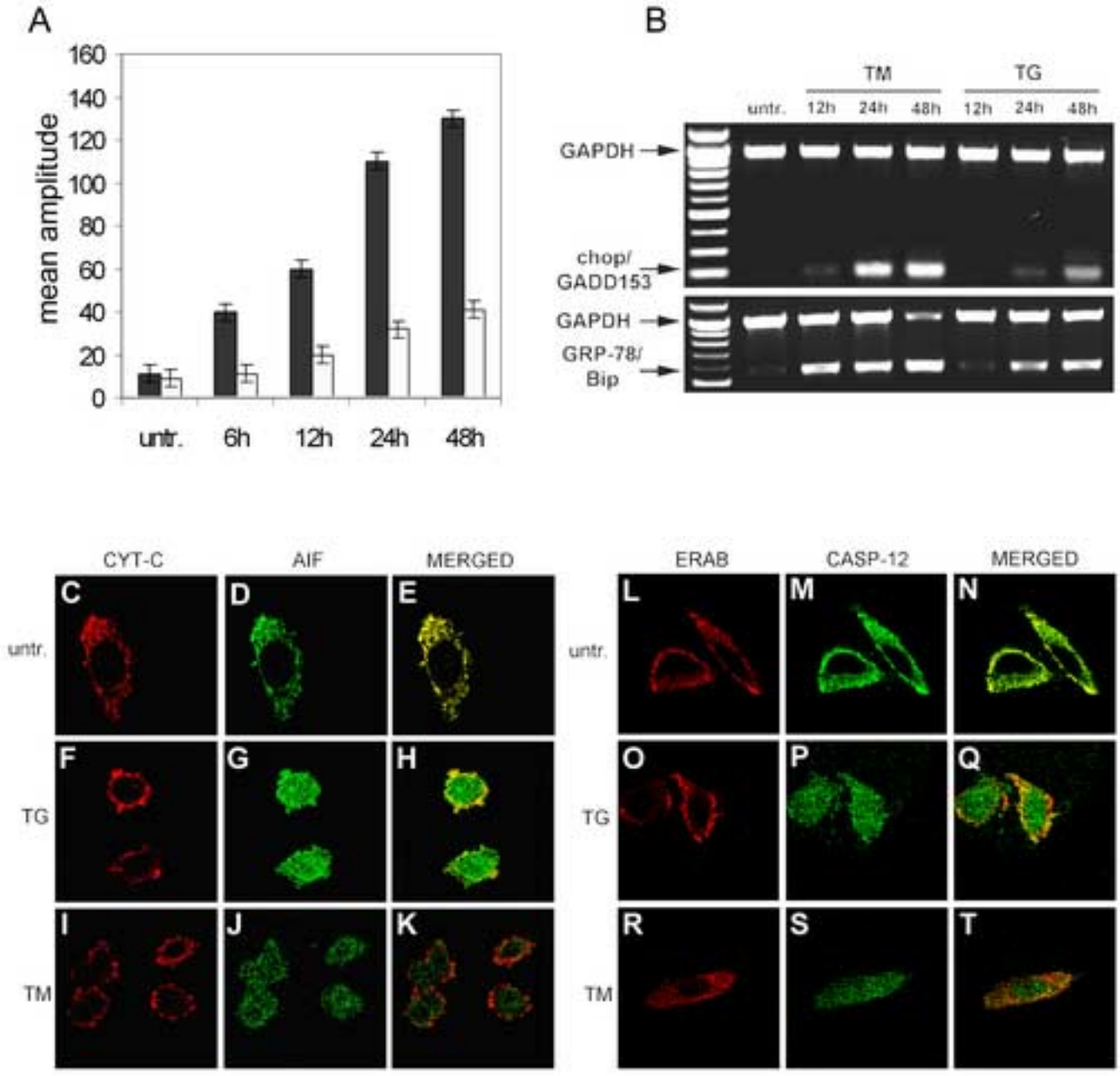

Figure 3

Click here to download high resolution image

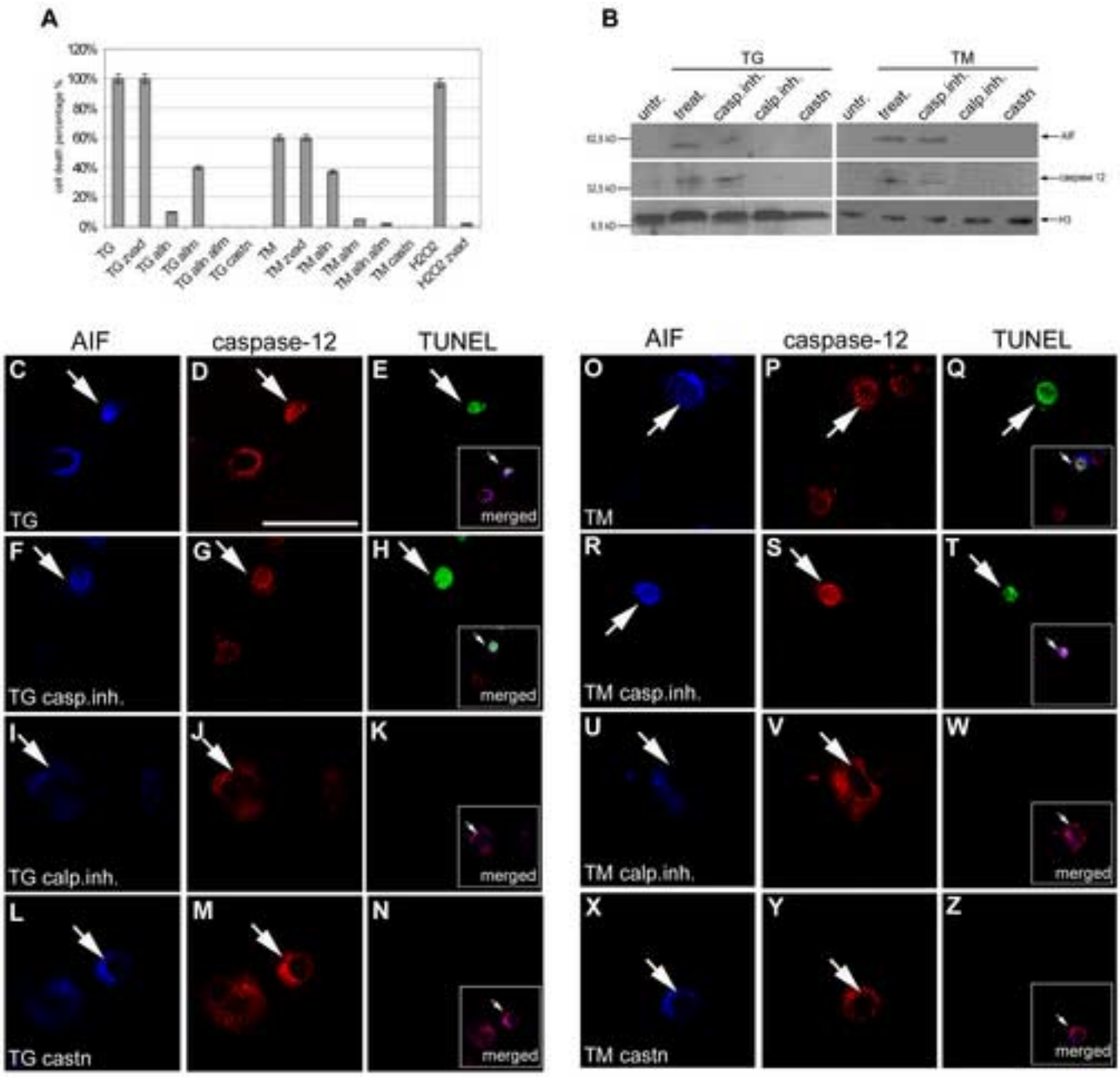

Figure 4

Click here to download high resolution image

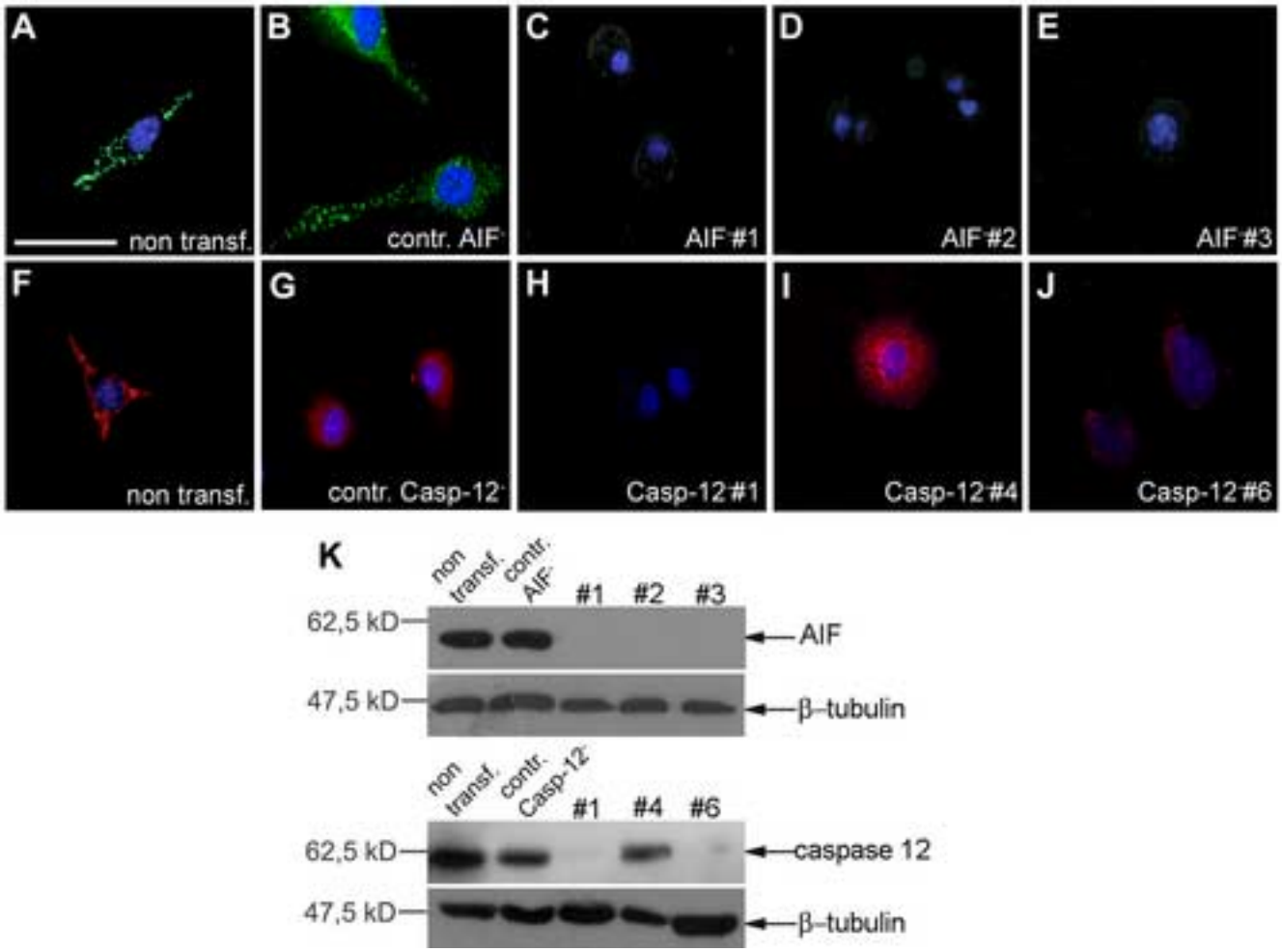

Figure 5

Click here to download high resolution image

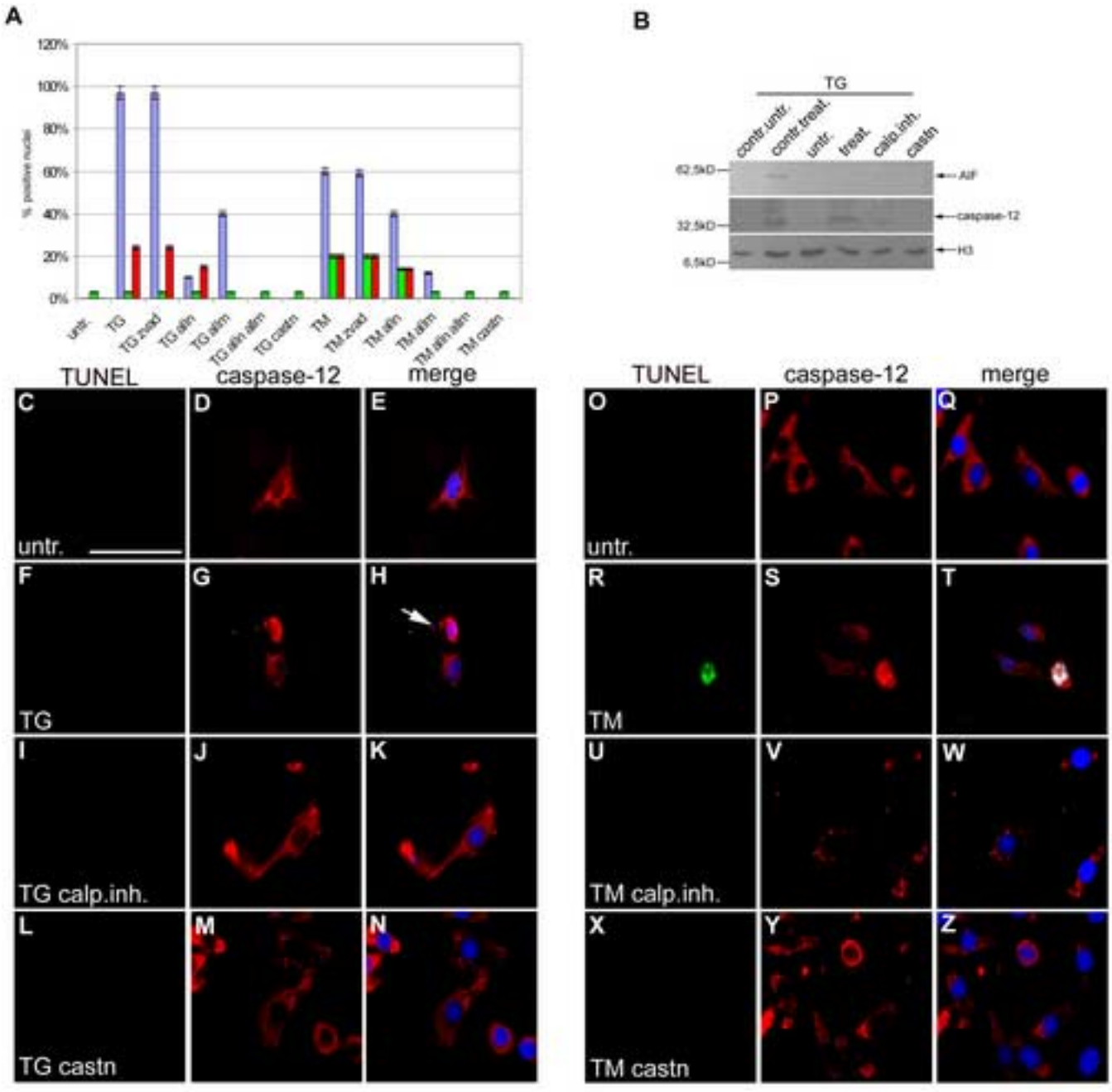

Figure 6

Click here to download high resolution image

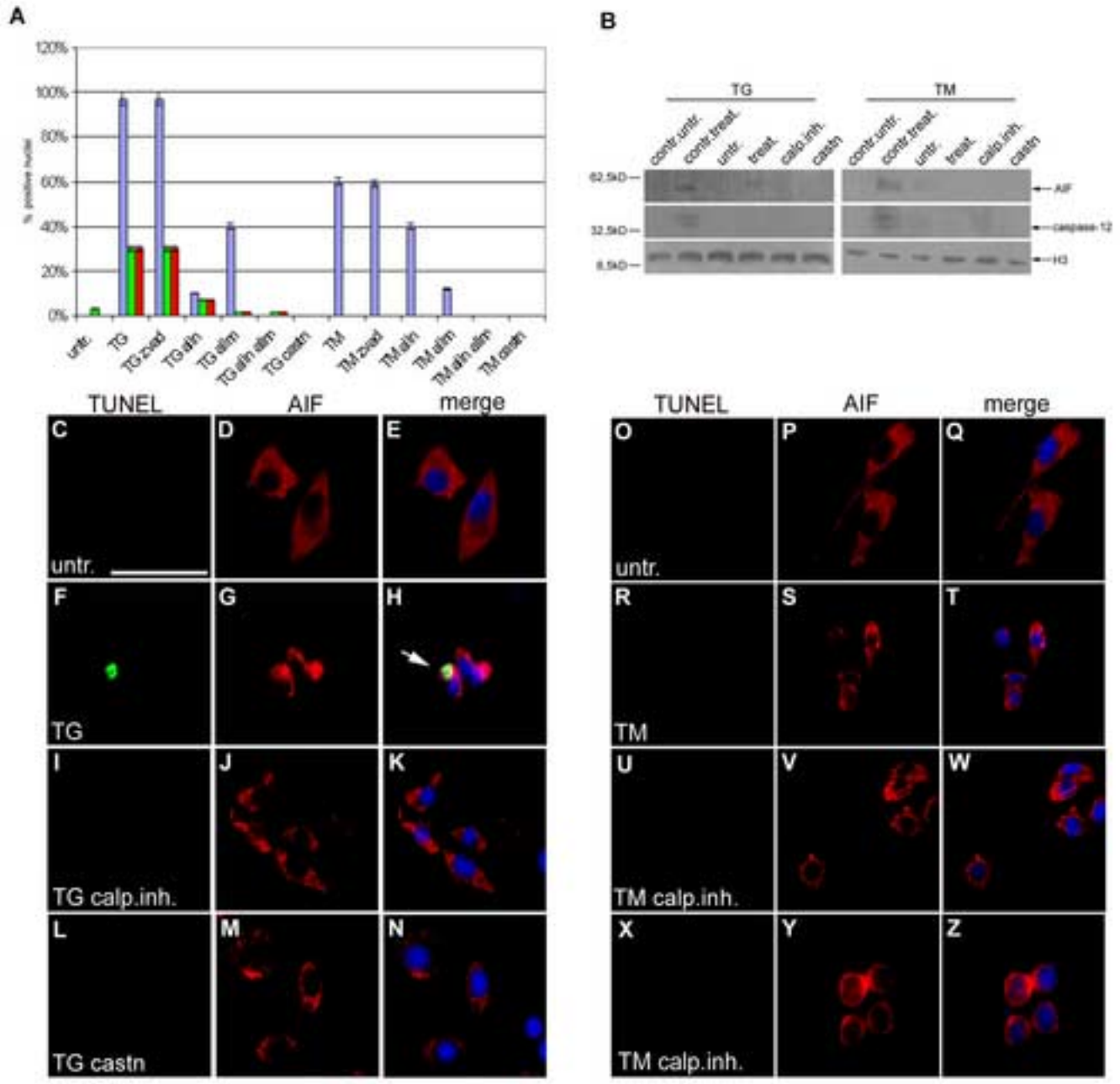

Figure 7

Click here to download high resolution image